Indian Journal of Pure & Applied Physics
Vol. 44, November 2006, pp. 820-825

Amplitude distribution analysis of acoustic emissions and investigation of the development of brittle fracture in rock

M V M S Rao & K J Prasanna Lakshmi

National Geophysical Research Institute, Hyderabad 500 007

Received 7 June 2005; revised 12 July 2006; accepted 3 August 2006

Materials undergoing brittle failure produce large number of acoustic emissions (AE) of varying amplitudes. The most useful way to describe and analyse the AE amplitude distribution is by computing the *b*-value (slope of the log-linear frequency-magnitude distribution of AE). Conventionally, the *b*-value of AE is calculated using the methods adopted in seismology since many similarities exist between AE and seismic waves. The *b*-value is usually obtained either from the cumulative frequency distribution or the discrete frequency distribution of earthquake magnitudes and the same principles hold good for the AE data also. We have carried out the AE amplitude distribution analysis using advanced software (Mistras-2001) and computed the AE *b*-value using the Gutenberg-Richter relationship for the cumulative frequency distribution data and Aki's method for the discrete distribution data. The results obtained by both these methods to evaluate the fracture process in a granite rock are compared and discussed as a case study in this paper. Useful inferences about the fractal distribution of crack lengths leading to the dynamic failure of the test rock could also be obtained using the AE *b*-value data.

Keywords: Microcracking, AE *b*-value, Rock fracture, Fractals
IPC Code: G10K11/16

1 Introduction

Materials undergoing brittle failure produce large number of acoustic emissions (AE) of varying amplitudes due to the formation and growth of micro-cracks, tensile cracks, shear cracks etc. The cumulative as well as the discrete frequency-amplitude distribution of such AE shows a descending gradient and a major portion of it is linear. The amplitude data of that linear range is used to compute the *b*-value (slope of the log-linear frequency-magnitude distribution of AE) following the Gutenberg-Richter relationship[1] for the cumulative frequency distribution data and Aki's method[2] for the discrete frequency distribution data. These two methods are still widely used in seismology[3]. The values of unity are quite common for both seismic *b*-value and AE *b*-value and it is a universal fact. The stress-induced changes and temporal variations in *b*-value have attracted the attention of both seismologists and materials scientists since many years and several interesting results also have been reported[3-15]. Some attempts have also been made in recent years to fine-tune the cumulative frequency - amplitude distribution graphs (data) and get the improved *b*-value (Ib-value) such that its variations may give a better insight into the fracture development processes in materials[16,17]. It involves filtering of high and low amplitude AE hits (or events) in a selective manner and also needs some corrections. In this paper, we have compared and discussed the results of *b*-values of AE which were obtained from the amplitude distribution analysis of AE that were recorded during the progressive failure of a granite rock under uniaxial compression in the laboratory.

2 Experimental Details

2.1 Data acquisition and replay of AE

We have carried out uniaxial compression tests and monitored the deformation and failure behaviour of set of Godhra granites from Panchamahals district, Gujarat. The tests were carried out by incrementing the stress at a constant rate on the test sample using a servo-controlled testing machine, and by recording the strain and AE concurrently[15]. The multi-parameter AE data including hits, ring-down counts and amplitudes was obtained using a PC-based AE system (Spartan of PAC, USA). The time duration of the test was 1080 s and the uniaxial compressive strength of the test sample was 229.27 MPa. We used a resonant type PAC AE sensor (freq.: 150 kHz) for data acquisition. The AE data files were processed using the *Mistras* software with the INI file that we have

specially designed for processing the AE hit-amplitude distribution data. The data reduction and evaluation of any desired set or subset of AE can be carried out using the graphs displayed on the screen and by enabling the 'overlay', 'graph expansion' and 'cursor' facilities. The user can position and shift the vertical and horizontal cursors for reading the data of each graph. An example of this is shown in Fig. 1(a and b) in which 4 sets of frequency distribution graphs of the peak amplitudes of AE hits are shown. The graphs were obtained during the replay of AE data. The discrete frequency distribution is shown as vertical bars and cumulative frequency distribution is shown as continuous line in Fig. 1(a and b). The frequency distribution graphs corresponding to the first 500 AE hits in the stress range of 0-30% failure stress are shown in Fig. 1(a), while those at the final failure corresponding to the stress range of 0-100% failure stress are shown in Fig. 1(b). We have used the 'pause' option at regular and discrete intervals during replay, and got the graphical display of both cumulative and discrete frequency distribution of several AE subsets as shown in Fig. 1 from the beginning until the end of each data file. The hit-amplitude data of each subset were obtained at 1 dB interval using the cursor facility, and the *b*-value of each subset was computed using Eqs (2) and (4) as follows.

2.2 Determination and analysis of AE *b*-value

2.2.1 Gutenberg-Richter relationship

The *b*-value is a parameter defined originally by Gutenberg and Richter[1] for estimating the likelihood of occurrence of earthquakes above a specified magnitude *M*. The equation is as follows:

$$\log_{10} N = a - bM \qquad \ldots(1)$$

where *M* is the Richter magnitude of earthquakes, *N* the incremental frequency (i.e., the number of earthquakes with magnitude greater than *M*), *a* is an empirical constant and *b* is the *b*-value which is mostly ~1.0. The standard error in *b* is $b/\sqrt{n}$ for a sample number of *n* earthquakes and 95% confidence limits are twice this value[2]. The Richter magnitude *M* is proportional to the logarithm of the maximum amplitude (A_{max}) recorded in a seismic trace and also to the logarithm of the source rupture[3] area (*S*). The Eq. (1) has been found to be valid for the AE data also after applying the necessary correction. The

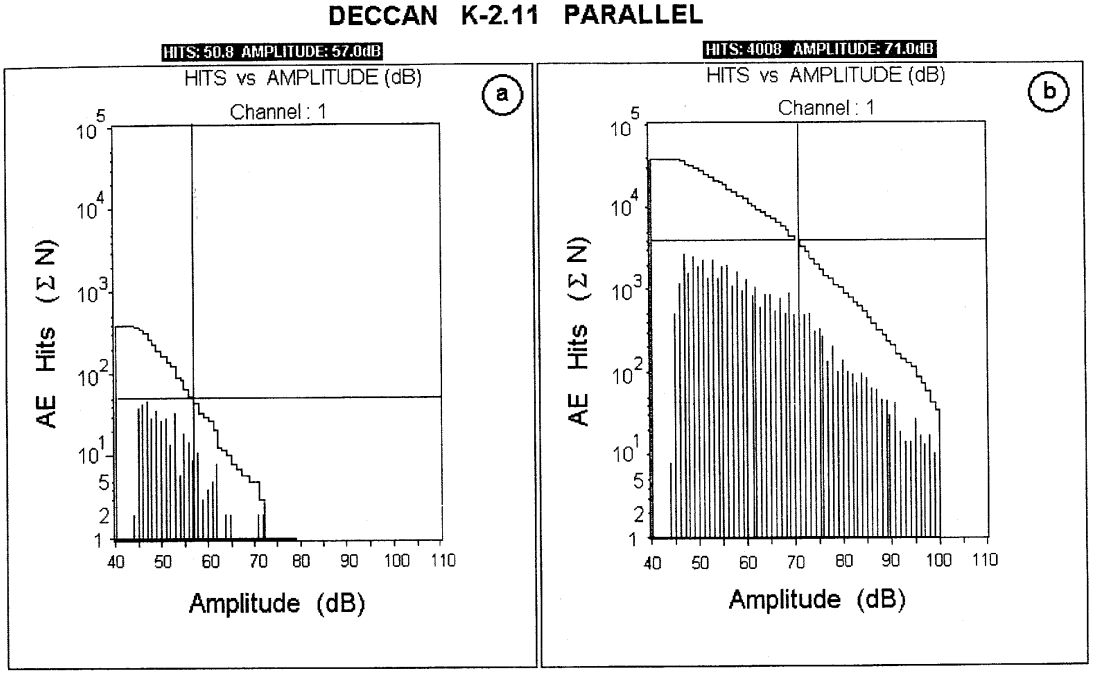

Fig. 1 — Hard copies of four frequency distribution graphs of the peak amplitudes of AE hits. The graphs were obtained from the replay of AE data that were recorded during the deformation and progressive failure of a granite rock (K-2.11) under uniaxial compression. The cumulative frequency distribution is shown as a continuous line and the discrete frequency distribution is shown as vertical bars, and both are shown together along with the vertical and horizontal cursors using the Mistras software. Plot (a) shows the distribution graphs corresponding to the first 500 AE hits in the stress range 0-30 % failure stress and plot (b) shows the distribution graphs corresponding to the total number of AE hits (58707) in the stress range 0-100% failure stress

correction factor is 20, and it arises because of the fact that the AE peak amplitude is measured in dB whereas the Richter magnitude of earthquake is defined in terms of the logarithm of maximum amplitude[8,9,11,13]. In terms of AE technique, the Gutenberg-Richter formula, therefore, gets modified as follows:

$$\log N = a - b\,(A_{dB}/20) \qquad \ldots(2)$$

where N is the incremental frequency (i.e., the number of AE hits or events with amplitude greater than the threshold A_T), a is an empirical constant and b is the b-value. The results obtained by this method are indexed as GBR values in Figs 2 and 3.

2.2.2 Aki's method

Aki introduced the 'Maximum likelihood method' which assigns an equal weighting to each recorded earthquake[2]. It takes only the discrete frequency distribution of earthquake magnitudes into account from which the b-value is computed as:

$$b = [\log_{10} e] \div [< m > - m_0] \qquad \ldots(3)$$

where e = 2.71828, b is the seismic b-value , $< m >$ is the average magnitude and m_0 is the threshold magnitude of the earthquakes that are recorded for a given area over a period of time. The Eq. (3) has been found to be valid for the AE data also after applying the correction factor to the AE amplitudes. The AE b-value can be computed as follows:

$$b = [20 \log_{10} e] \div [< a > - a_c] \qquad \ldots(4)$$

The mean amplitude $< a >$ of any given AE data set can be computed by using its statistical data of discrete frequency-amplitude distribution. The results obtained are indexed as Aki values in Figs 2 and 3.

3 Results and Discussion

3.1 Stress-induced changes in AE *b*-value

We have processed the peak amplitude data of nearly 40 sub-sets of AE in sequential non-overlapping time and stress-windows. The samples of graphs obtained are shown in Fig. 1(a and b). We have been able to compute the GBR b-value as well as Aki b-value using the methods as described above. The number of AE hits (samples) of each subset ranged between 50 and 500 for obtaining the amplitude distribution graphs and computation of b-value. The *b-value* of each subset when plotted against the applied stress gives valuable information about the changes in stress-induced microcracking in the test material as can be seen in Figs 2 and 3. Although major AE activity occurs at stresses ≥ 60% failure stress, the AE b-value plots are shown as a function of the whole stress (0-100% failure stress) in Fig. 2. During the early stages of loading (stage I), the AE generated due to the closure and rubbing of

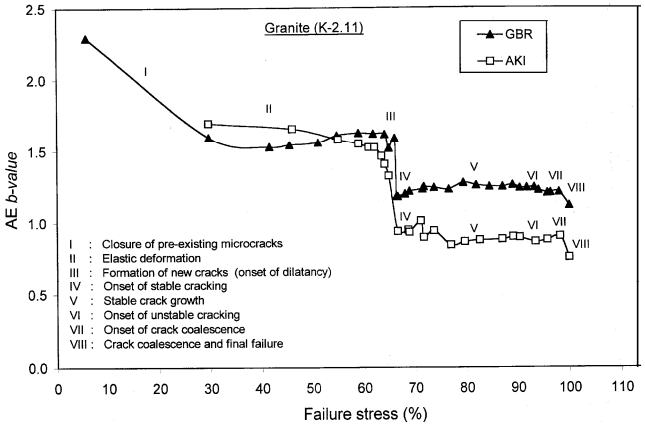

Fig. 2 — AE b-values obtained by using the Gutenberg-Richter relationship and Aki's method are plotted against stress (i.e., failure stress from 0-100%). The results were obtained from the replay of AE data (cumulative and discrete frequency distribution graphs of the peak amplitudes of AE hits) which was recorded during the deformation and progressive failure of a granite rock sample (No. K-2.11). The various stages at which sharp changes in AE b-value have occurred and the inferences drawn from them are also shown and listed in the in set

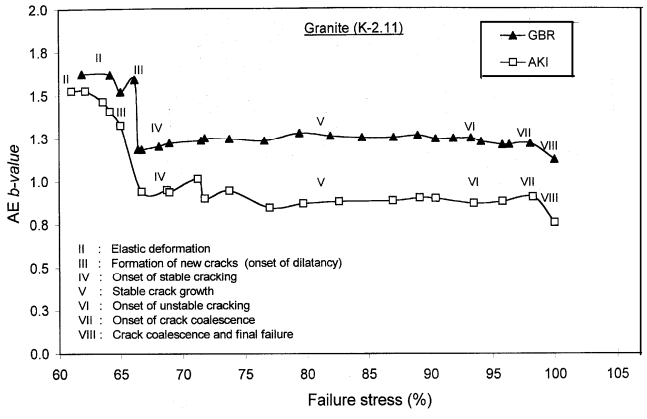

Fig. 3 — AE b-values obtained by using the Gutenberg-Richter relationship and Aki's method are plotted against stress (i.e., failure stress from 60-100%). The results were obtained from the replay of AE data (cumulative and discrete frequency distribution graphs of the peak amplitudes of AE hits) which was recorded during the deformation and progressive failure of a granite rock sample (No. K-2.11). The various stages at which sharp changes in AE b-value have occurred and the inferences drawn from them are also shown and listed in the set.

pre-existing microcracks in the rock began to show a high GBR *b*-value of 2.293 (stage I) and then it decreased to 1.532 and stabilized at that value during the elastic deformation stage (stage II) of the rock (Fig. 2). The Aki *b*-value was found to be 1.696 at the beginning of stage II and it had decreased to 1.527 at the end of that stage (Fig. 2). During these early stages, there were hardly any 'high amplitude' AE hits. Consequently, the *b*-values obtained by GBR method and Aki's method are close to each other during the elastic deformation stage. At the end of that stage, the dilatancy (inelastic volume change) began due to the formation of a large number of new microcracks which are perhaps distributed throughout in the test sample[15]. In the present study, it was found to be quite sudden and it took place at ~ 66% failure stress with *b*-value falling down sharply and also appreciably (GBR *b*-value from 1.522 to 1.183, Aki *b*-value from 1.465 to 0.940) during stage III (Fig. 2, Table 1). The GBR *b*-value is higher than Aki *b*-value owing to the fact that the AE population (cumulative in the case of GBR method and discrete in the case of Aki's method) always contains larger number of low amplitude AE hits. On account of this, the standard error ($b/\sqrt{n}$) in computing the *b*-value of individual sub-sets by GBR method is less compared to Aki's method (Table 1) since *n* is the number of AE hits. This is in total agreement with the results reported for earthquake *b*-values[2] and AE *b*-values[9].

Stage IV makes the beginning of transition from formation, to 'growth' stage of newly formed cracks. At the onset of stable cracking (i.e., stage IV), the *b*-value has increased to 1.222 (GBR method) and 0.950 (Aki's method) as shown in Fig. 3 and Table 1. During stage IV and also V, the newly formed cracks grow stably until their length is comparable to their spacing as a result of which the occurrence rate of AE decreases and a large number of AE would be of smaller amplitude. Therefore, the *b*-value increases slightly and may remain more or less steady as found in the present study (Fig. 3, Table 1) and also in our earlier work[11,12,14]. The onset of unstable cracking (stage VI) commenced with the release of some relatively high amplitude AE hits as a result of which the *b*-value has decreased until the applied stress reached a value of ≈ 97% failure stress. The coalescence of cracks commenced at that stage (VII) due to closer crack-spacing accompanied by the release of high amplitude AE hits. From then onwards the *b*-value began to decrease sharply due to crack-coalescence and accompanying stress relief, and at the final failure it decreased to as low as 0.759 (Aki's method), and 1.122 (GBR method). For all practical purposes, the transitions from stage V to stage VI and from stage VI to stage VII can be considered as most useful for the identification of critical state of damage and prediction of failure time of the test rock. At and around those critical stages, if the *b*-value can be determined for fixed number of hits with moving average window method, the results will be more advantageous. If the deforming test sample is allowed to undergo creep failure at that stage, it will be all the more better to investigate the micro-mechanics of rock fracture using AE data[12].

3.2 Mean crack length and fractal dimension

In the early stages of crack growth, there will be very little interaction among the individual cracks. But as the damage accumulates in the form of a fractal array of cracks, the crack density becomes critical and most of the neighbouring cracks begin to interact and nucleate leading to the formation of a large-scale shear or tensile fracture in the test rock. Since it is not possible to directly determine the crack

Table 1 — Statistics of AE *b*-values obtained by GBR and Aki's methods at the beginning of various important stages of stress-induced cracking as inferred from the AE data of test sample K-2 (Godhra granite)

Sl No	Feature	Stage No	Compressive Stress (% Failure stress)	AE *b*-value	
				GBR	Aki
1	Onset of the closure of pre-existing micro-cracks	I	5.79	2.293 ± 0.164	—
2	Onset of elastic deformation	II	29.67	1.600 ± 0.051	1.696 ± 0.088
3	Onset of dilatancy (formation of new cracks)	III	66.12	1.522 ± 0.019	1.465 ± 0.047
4	Onset of transition from 'formation' to 'growth'	III - IV	66.68	1.183 ± 0.010	0.940 ± 0.016
5	Onset of stable cracking	IV	68.95	1.222 ± 0.009	0.950 ± 0.016
6	Stable cracking in progress	V	82.63	1.263 ± 0.005	0.880 ± 0.007
7	Onset of unstable cracking	VI	94.09	1.249 ± 0.004	0.869 ± 0.006
8	Onset of crack coalescence	VII	98.26	1.216 ± 0.003	0.906 ± 0.006
9	Crack coalescence & final failure	VIII	100.00	1.122 ± 0.003	0.759 ± 0.004

density, the AE *b*-value monitoring can provide a means to estimate the mean crack length < *c* > and the fractal dimension of the crack length distribution (*D*) using the following equations[18] .

$$<c>=c_{min}[\{D/(D-1)\}][\{1-(c_{max}/c_{min})^{1-D}\}/\{1-(c_{max}/c_{min})^{-D}\}] \quad \ldots(5)$$

$$c_{max} = c_{min}[\{DN_T\}^{1/(D+1)}] \quad \ldots(6)$$

where c_{min} and c_{max} are the lower and upper bounds of the crack length, and N_T is the number of cracks in the population set of AE. The c_{min} is set by the threshold level of the detection of AE while c_{max} increases but remains finite[18,19]. By assuming further that direct proportionality exists between the measured AE event (or hit) rate N and the number of cracks N_T, and the *b*-value and fractal dimension *D*, the following relationships have been established[19].

$$N = 10^a = \lambda N_T \quad \ldots(7)$$

$$b = cD/3 \quad \ldots(8)$$

where *N* is the event rate (or hit rate) for occurrence above a threshold magnitude and N_T is the number of cracks, λ is the rate constant, a is an empirical constant and b is the *b*-value. The value of '*c*' depends on the time constants associated with the AE source and the recording instrument. For all practical purposes, it is assumed that λ = 1 and *c* = 1.5, which makes $N_T = N$, and D = 2*b*[19]. The experimental data of the present study when fitted into Eqs (5) to (8) has yielded useful results as shown in Fig. 4. It shows the plots of mean crack length (inferred) and fractal dimension as function of elapsed time. The deformation processes and various stages of development of the stress-induced cracks as inferred from these plots have been marked and shown in Fig. 4. The trends showing the increase in normalized mean crack length and decrease in fractal dimension D are more clearly seen at the beginning of stages III, VI and VII (Fig. 4). The phenomenal rise in crack population, mean crack length and the changing trends in the GBR *b-value* or *D* at stresses close to failure lead us to the conclusion that the onset of stage VI (i.e., onset of unstable cracking) as well as its transformation to stage VII (i.e., onset of crack coalescence) can be considered as the most crucial states of damage in rocks stressed to failure. If the incremental loading can be stopped at the critical stage of damage and the test sample is set to undergo creep failure, a better insight into the physics of rock fracturing can be gained using AE as reported recently by Lei *et al*[12]. Further the results will be more helpful if the *b*-value can be computed at those crucial

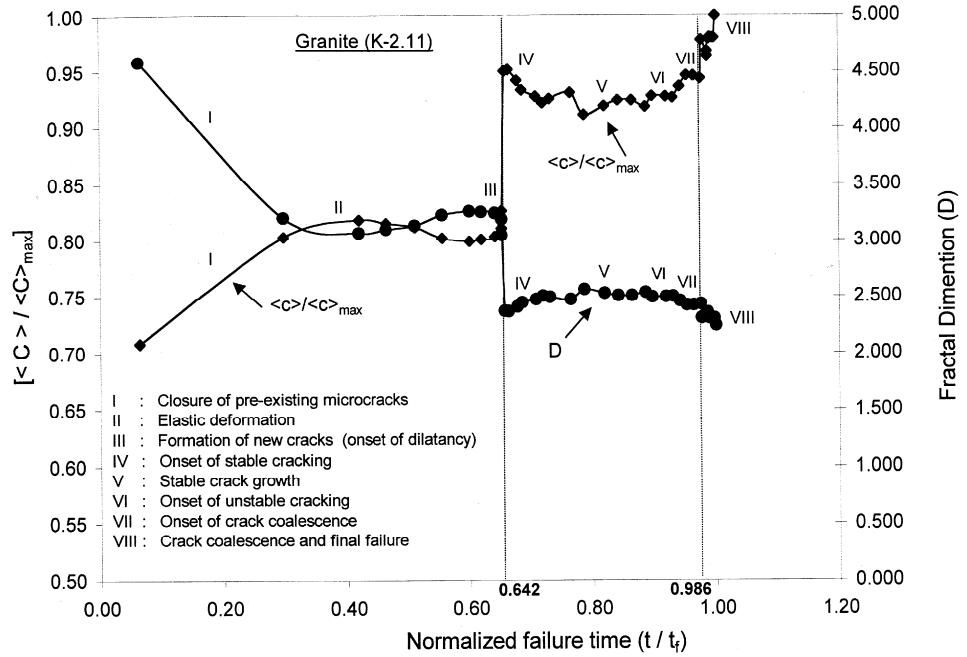

Fig. 4 — The inferred mean crack length (normalized) and observed fractal dimension (D=2*b*) are plotted as a function of normalized failure time. Sharp changes in them were found to occur at the onset of dilatancy (stage III, i.e., at 0.642 t_f) and at the onset of crack coalescence (stage VII, i.e., at 0.986 t_f) as inferred from the AE data of a granite rock

stages using the discrete frequency distribution data of AE amplitudes and the moving average window method. It could not be carried out for the present study.

4 Conclusions

1. The present study had shown that the AE technique combined with an advanced software such as Mistras-2001 can be used successfully to identify, track, analyse and characterize the various stages of the development of brittle fracture in materials such as rocks in terms of amplitude distribution and AE *b*-value.
2. The computation of *b*-value from the cumulative and discrete frequency distribution graphs and the comparison of results has been found to be helpful. With the increase of AE population at stresses close to failure, the discrete frequency distribution of AE amplitudes yielded lower AE *b*-values (Aki) than the cumulative frequency distribution data (GBR). However the trends of the precursory changes in AE *b*-value (GBR) and (Aki) were found to be identical.
3. The AE sampled and characterized in terms of *b*-value at stresses close to failure clearly indicated the onset of unstable cracking and also that of crack coalescence leading to dynamic failure of the test rock. These observations have some vital applications for monitoring the stability and integrity of rock at several scales.
4. A quantitative assessment of fracture development in brittle rock in terms of mean crack length (normalized) and fractal dimension of the crack size distribution could also be made using the AE *b*-value data.

Acknowledgement

This forms a part of the project funded by the Department of Science & Technology, Government of India. The authors are thankful to Dr. V.P. Dimri, Director, NGRI, Hyderabad and Dr. R.N. Gupta, Director, NIRM for extending all the facilities and according permission to publish this paper. We are thankful to the anonymous reviewer for making useful suggestions which have improved the presentation and discussion of results.

References

1 Gutenberg B & Richter C F, *Seismicity of the Earth and Associated Phenomena* (2nd edn.), Princeton University Press, Princeton, NJ, USA, (1954) 310.
2 Aki K, *Bull Earthquake Res Inst,* Tokyo University, 43 (1965) 237.
3 Shearer P M, Introduction to seismology. *Cambridge Univ Press,* Cambridge, England, (1999) 1-189.
4 Mogi K, *Bull Earthquake Res Ins Tokyo Univ*, 40 (1962) 831.
5 Scholz C H, *Bull Seis Soc Am,* 58 (1968) 399.
6 Meredith P G & Atkinson B K, *Geophys J R astr Soc,* 75 (1983) 1.
7 Sammonds P R, Meredith P G & Main I G, *Nature*, 359 (1992) 228.
8 Cox S J D & Meredith P G, *Int J Rock Mech Min Sci Geomech Abstr,* 30(1) (1993) 11.
9 Hatton C G, Main, I G & Meredith P G, *J Struct Geol,* 15 **(**1993) 1485.
10 Lockner D, *Int J Rock Mech Min Sci,* 30 (1993) 883.
11 Rao M V M S, *Proc. 14th World Conference on Non-Destructive Testing (14th WCNDT), New Delhi, India, Dec. 1996,* (eds) C.G. Krishnadas Nair *et al*., Oxford & IBH Publ., New Delhi, 4 (1996) 2463.
12 Lei X, Kusunose K, Rao M V M S, Nishizawa O & Satoh T, *J Geophys Res*, 105(B3) (2000) 6127.
13 Colombo I S, Main I G & Ford M C, *J Materials in Civil Eng*, 15 (3) (2003) 280.
14 Rao M V M S, Adesh Kumar, Murthy D S N, Nagaraja Rao G M, Udaya Kumar S & Mohanty S K, *J Ind Geophys Union*, 5 **(**2001) 83.
15 Rao M V M S, Murthy D S N, Nagaraja Rao G M, Mohanty, S K & Udaya Kumar S, *J Geol Soc Ind*, 64 (2004) 775.
16 Shiotani T, Yuyama S, Li Z W & Ohtsu M, *J Acoustic Emission*, 19 (2001) 118.
17 PAC 2002, *b*-Value Software Option. User's Manual. Manual released by the Physical Acoustics Corporation, USA (2002).
18 Main I G, *Geophys J Int*, 107 (1991) 353.
19 Main I G & Meredith P G, *Geophys J Int*, 107 (1991) 363.